RESEARCH ARTICLE

Gammaherpesvirus Infection of Human Neuronal Cells

Hem Chandra Jha,[a] Devan Mehta,[a] Jie Lu,[a] Darine El-Naccache,[a] Sanket K. Shukla,[a] Colleen Kovacsics,[b] Dennis Kolson,[b] Erle S. Robertson[a]

Department of Microbiology and the Tumor Virology Program, Abramson Cancer Center, Perelman School of Medicine at the University of Pennsylvania, Philadelphia, Pennsylvania, USA[a]; Department of Neurology, Perelman School of Medicine at the University of Pennsylvania, Philadelphia, Pennsylvania, USA[b]

H.C.J. and D.M. contributed equally to this work.

ABSTRACT **Gammaherpesviruses human herpesvirus 4 (HHV4) and HHV8 are two prominent members of the herpesvirus family associated with a number of human cancers. HHV4, also known as Epstein-Barr virus (EBV), a ubiquitous gammaherpesvirus prevalent in 90 to 95% of the human population, is clinically associated with various neurological diseases such as primary central nervous system lymphoma, multiple sclerosis, Alzheimer's disease, cerebellar ataxia, and encephalitis. However, the possibility that EBV and Kaposi's sarcoma-associated herpesvirus (KSHV) can directly infect neurons has been largely overlooked. This study has, for the first time, characterized EBV infection in neural cell backgrounds by using the Sh-Sy5y neuroblastoma cell line, teratocarcinoma Ntera2 neurons, and primary human fetal neurons. Furthermore, we also demonstrated KSHV infection of neural Sh-Sy5y cells. These neuronal cells were infected with green fluorescent protein-expressing recombinant EBV or KSHV. Microscopy, genetic analysis, immunofluorescence, and Western blot analyses for specific viral antigens supported and validated the infection of these cells by EBV and KSHV and showed that the infection was efficient and productive. Progeny virus produced from infected neuronal cells efficiently infected fresh neuronal cells, as well as peripheral blood mononuclear cells. Furthermore, acyclovir was effective at inhibiting the production of virus from neuronal cells similar to lymphoblastoid cell lines; this suggests active lytic replication in infected neurons *in vitro*. These studies represent a potentially new *in vitro* model of EBV- and KSHV-associated neuronal disease development and pathogenesis.**

IMPORTANCE **To date, no *in vitro* study has demonstrated gammaherpesvirus infection of neuronal cells. Moreover, worldwide clinical findings have linked EBV to neuronal pathologies, including multiple sclerosis, primary central nervous system lymphoma, and Alzheimer's disease. In this study, for the first time, we have successfully demonstrated the *in vitro* infection of Sh-Sy5y and Ntera2 cells, as well as human primary neurons. We have also determined that the infection is predominately lytic. Additionally, we also report infection of neuronal cells by KSHV *in vitro* similar to that by EBV. These findings may open new avenues of consideration related to neuronal pathologies and infection with these viruses. Furthermore, their contribution to chronic infection linked to neuronal disease will provide new clues to potential new therapies.**

Received 25 October 2015 **Accepted** 28 October 2015 **Published** 1 December 2015

Citation Jha HC, Mehta D, Lu J, El-Naccache D, Shukla SK, Kovacsics C, Kolson D, Robertson ES. 2016. Gammaherpesvirus infection of human neuronal cells. mBio 6(6):e01844-15. doi:10.1128/mBio.01844-15.

Editor Glen Nemerow, Scripps Research Institute

Address correspondence to Erle S. Robertson, erle@mail.med.upenn.edu.

This article is a direct contribution from a Fellow of the American Academy of Microbiology.

Epstein-Barr virus (EBV) is a highly ubiquitous herpesvirus, asymptomatically infecting 90 to 95% of adults worldwide regardless of demographics or location. Classified as a human gammaherpesvirus (human herpesvirus 4), EBV is a large double-stranded DNA virus known to infect primarily B lymphocytes (1–4). The virus can also infect other lymphocytes and certain types of epithelial cells (5–7). EBV is transmitted through the exchange of bodily fluids and is most commonly known as the cause of infectious mononucleosis (8, 9). The virus is also associated with a number of human cancers, including Burkitt's lymphoma and nasopharyngeal carcinoma (10–12). We also examined another member of the *Gammaherpesviridae* family known as Kaposi's sarcoma (KS)-associated herpesvirus (KSHV) that is associated with KS, multicentric Castleman's disease (MCD), and primary effusion lymphoma (PEL) (13, 14).

EBV binds to B lymphocytes through the interaction of viral glycoprotein gp350/220 with the cellular receptor CD21 (15). Subsequently, fusion of the viral envelope with the cell membrane occurs, allowing the virus to enter the host (16). In order to infect epithelial cells, it is believed that the viral protein BMRF-2 interacts with β1 integrins, initiating fusion between the viral envelope and cellular membrane (17, 18).

After infection of B lymphocytes or epithelial cells, EBV initiates either latent (nonproductive) or lytic (productive) replication. Latently infected cells maintain EBV genomes as 184-kb episomes and express a limited repertoire of viral gene products (4). In latent infection, among the most commonly expressed viral genes are six nuclear antigens (EBNA1, -2, 3A, 3B, -3C, and -LP), three membrane-associated proteins (LMP-1, -2A, -2B), and two small noncoding RNAs (EBER1 and EBER2) (10, 19, 20). There

are four known latency programs associated with EBV in which the expression patterns of these genes are altered (3). EBNA1, which binds to the origin of latent replication on the viral genome, mediates replication of the episome during mitosis of the host cell. It is expressed in all latency programs and is therefore a beneficial target to determine infection (21).

Similar to those seen in KS and PEL, KSHV genomes are detectable in almost all HIV-seropositive MCD cases and approximately 50% of HIV-seronegative MCD cases (22, 23). Interestingly, and different from PEL cells, coinfection of EBV with KSHV has not been detected in MCD plasmablasts. Generally, three viral gene products are clearly expressed in all latently infected cells from a single promoter in a tricistronic transcript, i.e., LANA, vCYC, and vFLIP (24). However, other viral gene products are expressed in different lymphoproliferative disorders (24, 25). K8 is a replication-associated protein and is also characterized as a delayed early lytic antigen, as it is expressed after RTA (open reading frame 50) (26).

In lytic infection, viral genes selectively replicate virion genomes, which causes release of viral particles from the host cell. In B cells, lytic replication generally occurs after reactivation from the latent phase, while in epithelial cells, lytic replication occurs for a short period initially after infection, eventually returning to the latent phase (6, 27). The mechanism of reactivation in both B and epithelial cells is not specifically understood. However, *in vitro*, reactivation can be initiated by treating cells with sodium butyrate and 12-*O*-tetradecanoylphorbol-13-acetate (TPA) (28). The viral genes expressed during lytic replication include those for glycoprotein 320/220, BZLF-1, RTA, and K8, a transcriptional activator that facilitates reactivation (29, 30).

In addition to its association with several lymphoproliferative diseases, EBV is clinically linked to a wide range of neural ailments, such as primary central nervous system (CNS) lymphoma, multiple sclerosis (MS), Alzheimer's disease, cerebellar ataxia, subacute sensory neuropathy, meningoencephalitis, cranial nerve palsies, and Guillain-Barré syndrome (31–40). The association of EBV with these diseases is based largely on the fact that cerebrospinal fluid (CSF) samples from neurologically compromised patients contain unusually high EBV titers. As a result, testing of the CSF of patients evaluated for neurological disease for EBV is becoming more common (41, 42).

Among the neural ailments with possible links to EBV, MS, a chronic inflammatory demyelinating disease of the CNS, has more recently become a focus of study (43). In 1979, Fraser and others reported that for patients with clinically active MS, peripheral blood lymphocytes have an increased tendency toward spontaneous EBV-induced lymphocyte transformation (44). Later, Sumaya and colleagues reported higher seropositivity and higher serum anti-EBV titers in MS patients than in controls (45). More recently, Munger et al. concluded that, "anti-EBNA antibodies are strong, robust markers of MS risk and could be useful in MS risk score" (34). They also showed that MS rates tend to rise significantly in patients who have been exposed to EBV infection characterized by infectious mononucleosis (34). In addition, individuals who are still EBV seronegative in adulthood are potentially resistant to both MS and EBV infection (46). Interestingly, MS patients also have an increased and broad frequency of $CD4^+$ cells recognizing EBNA1 (33, 34, 47–50). Further, in 2007, Serafini and colleagues reported that EBV-positive B cells and plasma cells were found in the brains of 21 of 22 MS patients, confirming the presence of the virus in the brain (51). In terms of disease management, acyclovir (ACV), an antiviral drug used to treat herpesvirus, including EBV, infections, has been shown to significantly inhibit triggering of MS exacerbations, suggesting that an ACV-susceptible virus might be involved in the pathogenesis of MS (9, 52–54). Although EBV has certainly not been proven to be the cause of MS, there is some level of correlation. Whether the virus is causative, contributing, or present in the microenvironment that provides a perfect niche for survival has yet to be fully investigated. Additionally, there is no previous study relating KSHV infection with neuronal cell infection.

It is evident that EBV is associated with neurological complications and diseases. While some of these associations have been developed more than others, it is important to note that the research has not thoroughly investigated the possible molecular mechanisms that would solidify the relationship between the oncogenic gammaherpesvirus with CNS-associated diseases. It is known that EBV can be present in the CNS, in infected B cells or plasma cells, or in the CSF of neurologically affected patients (55). Is it therefore possible that the presence of EBV or KSHV in the brain and periphery may be a result of direct infection of neuronal tissue, more specifically, neurons themselves? If so, what are the characteristics of this infection? Is the infection similar to the latency and transformation programs seen in B cells or epithelial cells? Or does the virus in neurons undergo a transcription program distinct from what is known of EBV or KSHV during infection *in vitro*?

This study had two broad aims. First, this work has established that EBV and KSHV can infect neuronal cells. Second, this study has characterized the properties of the infection. If the presence of EBV and KSHV in the CNS can be further explored, then this will enhance our understanding of neurological pathologies and the associations or potential contributions of viral and other infectious agents in the future.

In this study, we infected the Sh-Sy5y human neuroblastoma cell line, differentiated teratocarcinoma Ntera2 (NT-2) neurons, and primary human fetal neurons with recombinant virus containing the gene for green fluorescent protein (GFP) (52). GFP fluoresces when exposed to light at a wavelength of 542 nm in human cells and can be monitored via noninvasive methods. Postinfection of the three neuronal cell types, we monitored cell density, morphology, and viral gene expression via reverse transcriptase quantitative PCR (RT-qPCR) and Western blot (WB) analyses. In the Sh-Sy5y cell line and in primary human fetal neurons, we examined viral protein production by immunofluorescence methods. After infection was confirmed, we investigated the characteristics of the infection by analyzing viral gene expression trends postinfection of fresh Sh-Sy5y cells and peripheral blood mononuclear cells (PBMCs) by using supernatant from infected cells. We also examined whether ACV has any effect on the proliferation of Sh-Sy5y cells infected with virus generated from infected Sh-Sy5y cells versus that from lymphoblastoid cell line 1 (LCL1).

RESULTS

Neuronal cell lines can be infected by EBV. To determine if EBV can infect neural cells, we exposed Sh-Sy5y cells, differentiated NT-2 neurons, and primary human fetal neurons to a strain of genetically modified EBV that expresses GFP, GFP-EBV (52).

Sh-Sy5y cells were generated from a bone marrow biopsy spec-

imen from a 4-year-old girl with neuroblastoma (56). These cells were established as neuroblastoma and epithelium-like cells (57). NT-2 was initially isolated from a lung metastasis of a 22-year-old male with primary embryonal carcinoma of the testis (58). NT-2 cells show properties of early embryo cells and can be used to study the early stages of human neurogenesis (59). Human primary neurons were collected from brain tissue obtained from fetuses aborted early in the second trimester of gestation. These procedures were performed in full compliance with National Institutes of Health and Temple University ethical guidelines (60).

After 24 h, cells were monitored via fluorescence microscopy for up to 9 days postinfection (dpi) at specified time intervals. Cells were collected from all assays, and RNA was extracted for quantitative determination by RT amplification of viral genes. The Sh-Sy5y neuroblastoma cell line expressed GFP as early as 1 dpi, indicating that the cells were successfully infected and that the viral genome was being transcribed and translated (Fig. 1A to E). In the first few days of infection, only about 10 to 20% of the cells expressed GFP. However, the percentage of cells expressing GFP increased as the infection progressed. About 90 to 95% of the cells expressed GFP by day 9. Interestingly, as the cells progressed toward 9 dpi, their overall density decreased and cell lysis was observed. Furthermore, after EBV infection, the morphology of infected Sh-Sy5y cells was distinct from that of uninfected cells. While uninfected cells had a characteristic triangular shape, infected cells had a swollen, rounder shape and displayed longer, more defined neural processes in the two sets of infections (Fig. 1A, left and right sides).

Total RNA was collected from the cells and reverse transcribed to cDNA before a qPCR assay was carried out with the cDNA generated from infected Sh-Sy5y cells. The genes amplified were the EBV latent genes for EBNA1 and EBNA3C, the EBV early lytic gene for BZLF1, and the major lytic gene for gp350 (Fig. 1B to E). The gene for glyceraldehyde 3-phosphate dehydrogenase (GAPDH) was used as an endogenous control. As shown in Fig. 1B, EBNA1 showed significant expression, which confirmed the infection and latent gene expression from the viral genome. The genes for EBNA3C, BZLF1, and gp350 displayed a significant amount of amplification, which was maximal at 5 dpi with the gene for EBNA3C and decreased at 7 and 9 dpi (Fig. 1C to E). EBNA1 signals continued to increase, and BZLF1 and gp350 signals increased steadily up to 5 dpi and then plateaued at 7 to 9 dpi (Fig. 1B to E).

NT-2 cells expressed characteristics similar to those of Sh-Sy5y cells postinfection with GFP-EBV (Fig. 2). These neurons, prior to infection, form clusters containing many cells. These clusters are composed of cell bodies, while the axons protrude from the clusters to join with other nearby cells and clusters. After infection with GFP-EBV, NT-2 neural cells also expressed GFP by 24 h postinfection, as determined by green fluorescence. At that point, 95 to 100% of the neural clusters express some level of GFP (Fig. 2). Initially, in the first few days, the GFP signals were isolated toward the outside rim of the cell clusters, forming a green fluorescent halo or ring, as shown by microscopy (Fig. 2). This suggests that the cells in the outer layer of these clusters are likely the first to become infected because they are in direct contact with the virus. However, as the infection progressed, the green fluorescent signal gradually migrated toward the core of the clusters, and by 6 dpi, all of the cells in the neural clusters were infected, as determined by green fluorescence assay. Furthermore, the clusters became distinctively darker and swollen, indicating that they are undergoing cell death. Interestingly, at 9 dpi, no living cells remained in the culture, as determined by trypan blue staining and microscopy. Floating cell debris was mostly observed, with some expressing GFP.

Similar to Sh-Sy5y cells and NT-2 neurons, primary human fetal neurons also expressed strong GFP signals after incubation with GFP-EBV *in vitro* (Fig. 3). The GFP signals were observed in 70 to 80% of the cells at 48 h postinfection (2 dpi, Fig. 3). As the infection progressed, the GFP-expressing cells became deformed with uncharacteristic swelling. This was followed by a decrease in the percentage of GFP signals from the infected neurons by day 4 postinfection. The GFP signals were clearly seen in the cell bodies, as well as the axons, and the most intense GFP signals were seen at the cell body. At 8 dpi, the majority of the cells had lost their membrane integrity and most of the GFP signal (Fig. 3). This suggested that infection had occurred in a manner similar to that seen in the Sh-Sy5y and NT-2 neuronal cell lines.

Characterization of viral gene expression in infected neurons. We selected Sh-Sy5y cells and primary human fetal neurons for gene expression. Immunofluorescence analyses were carried out temporally to examine the level of virus-encoded antigens in the infected cells after EBV infection. In our assays, viral GFP was examined while 4′,6-diamidino-2-phenylindole (DAPI) staining was used as a nuclear control. Two EBV antigens, latent EBNA1 and lytic gp350, were targeted to validate infection (Fig. 4).

Infected Sh-Sy5y cells at 24 h showed a strong GFP signal with a punctate EBNA1 signal localized in the nucleus (Fig. 4A). As the infection progressed, this signal became stronger with an exclusive nuclear localization. This undoubtedly indicated that EBV infection was successful. We also monitored late lytic EBV glycoprotein gp350 (Fig. 4A). Gp350 is a membrane protein (61) and therefore would localize to the outer cell membrane. This localized expression was seen predominantly at the cell membrane by 7 and 9 dpi (Fig. 4A). Therefore, infected cells were producing EBV late antigens.

To further characterize EBV latent and lytic gene expression during this early period of infection, we performed WB analyses for the essential latent antigen EBNA1 and the immediate-early transcription activator BZLF1. Our results confirmed that weak EBNA1 signals were detected at 24 h and their strength increased by 48 h (Fig. 4B). Interestingly, BZLF1 signals were seen as early as 48 h postinfection and remained at a consistent level up to 9 dpi (Fig. 4B). The GAPDH control blot was used as a loading control.

Primary human fetal neurons also expressed the EBNA1 and BZLF1 proteins, as was clearly shown by immunofluorescence assays from day 2 onward (Fig. 5A and B). The EBNA1 protein signal was localized predominantly in the nucleus, as expected for this nuclear antigen. To determine if the infected cells were neuronal cells, we used the neuronal marker MAP2 (62). As shown by our immunofluorescence assay results, MAP2 staining was clearly observed, demonstrating that these cells were infected neuronal cells (Fig. 5A and B).

We monitored the expression profile of the viral genes for the latent proteins EBNA1 and EBNA3C, as well as major lytic glycoprotein gp350 and immediate-early lytic antigen BZLF1. The RT-qPCR results demonstrated that by 24 h postinfection (1 dpi), EBNA1 and EBNA3C were clearly detected, with maximal EBNA1 levels at 48 h and a plateau at 72 h postinfection (3 dpi) to 9 dpi (Fig. 5B). However, EBNA3C and BZLF1 levels were slowly re-

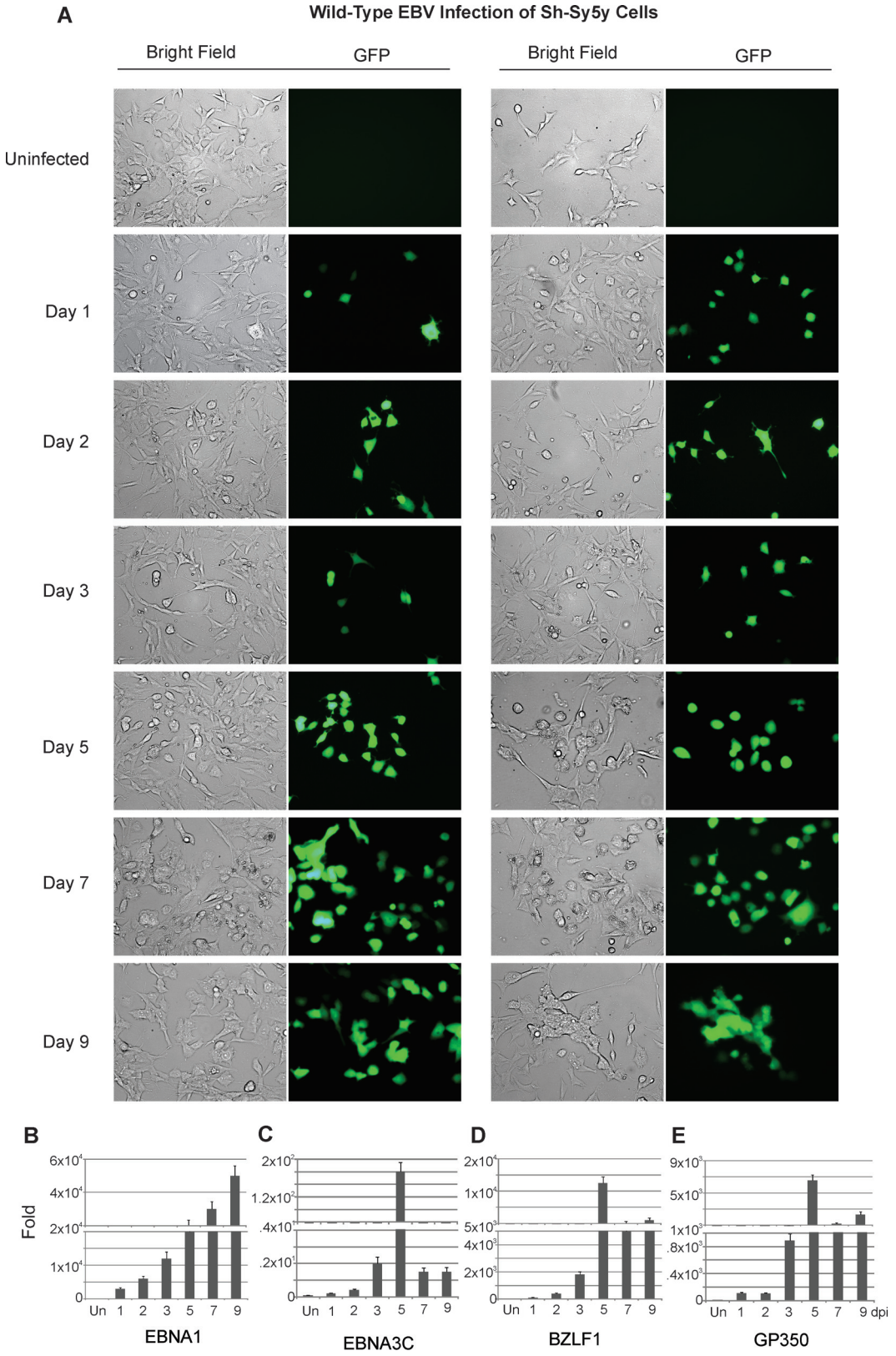

FIG 1 Wild-type EBV infection of Sh-Sy5y cells. Sh-Sy5y cells were grown on 100-mm culture plates. At 60% confluence, in addition to the culture medium, 110 μl (~6 × 10^{12} viral copies) of concentrated EBV was added to each plate with 5 μl of Polybrene at a 20-μmol/ml concentration. Control cells were supplemented with only medium and Polybrene. (A) Fluorescence microscopy was carried out at 1, 3, 5, 7, and 9 dpi to monitor GFP expression. (B to E) Cells were harvested at 1, 2, 3, 5, 7, and 9 dpi for EBNA1, EBNA3C, BZLF1, and gp350 transcript analysis. Microscopy images were captured at ×20 magnification.

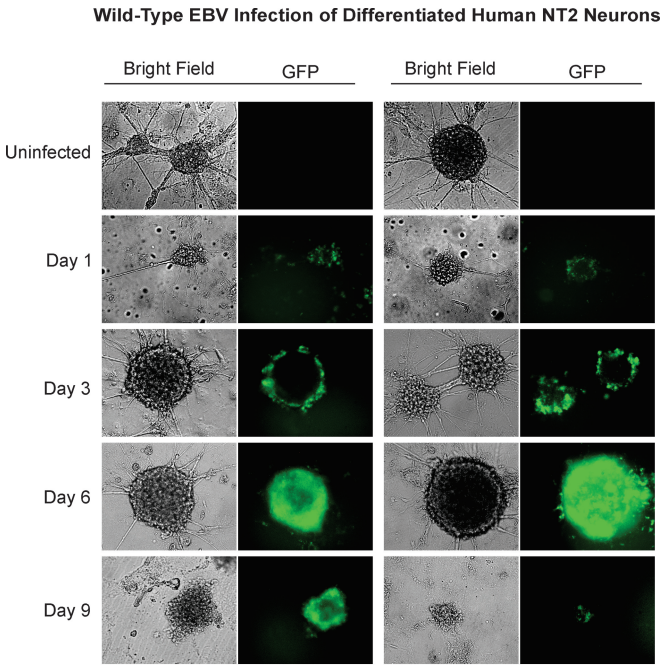

FIG 2 Wild-type EBV infection of differentiated human NT-2 neurons. NT-2 neurons were differentiated in six-well plates at a density of 700 to 900 neural clusters per well. In addition to 2 ml of complete culture medium per well, 100 μl (~5.5 $\times$ 10^{12} viral copies) of concentrated virus was added. The medium was changed every 3 days. Fluorescence microscopy was carried out at 1, 3, 6, and 9 dpi to monitor for GFP expression. Microscopy images were captured at $\times$20 magnification.

duced after day 5. Gp350 showed a gradual increase in expression of the transcripts, which continued up to 9 dpi (Fig. 5C).

EBV produced from Sh-Sy5y can infect neuronal cells and PBMCs. To determine if EBV undergoes latent or lytic replication and produces progeny virus in neuronal cells, we collected the supernatant from Sh-Sy5y cells infected with GFP-EBV at 2, 5, and 9 dpi. The virus collected was filtered with a 0.45-μm filter and concentrated by ultracentrifugation. The filtered supernatant was used to infect fresh Sh-Sy5y cells and PBMCs to determine if virus was produced. Microscopy was performed at 2 and 5 dpi, and a qPCR assay was performed with DNA extracted from cells infected with GFP-EBV. The results of incubation with supernatant from the initial EBV-infected Sh-Sy5y cells and qPCR for EBV-DNA with primers to detect EBNA1 show that fresh Sh-Sy5y cells were positive for EBV genomes (Fig. 6A and C). The infection efficiency was similar in all newly infected cells, and the trend and the intensity of the infection were similar for viral supernatants collected at days 2, 5, and 9 from Sh-Sy5y cells and PBMCs (Fig. 6A). At day 5, the majority of the cells showed a GFP signal that was weaker at 2 dpi (Fig. 6A). However, by day 5, the GFP signal and infection were visibly increased (Fig. 6A, right side). RT-qPCR for EBNA1 DNA to confirm infection showed no significant difference between the supernatants used (Fig. 6A and C).

Infected PBMCs displayed results similar to those obtained with the Sh-Sy5y cell line (Fig. 6B and D). The infection signal was weaker at day 2 with supernatant collected at 2, 5, and 9 days and increased substantially at 5 dpi (Fig. 6B and D). Interestingly, the levels of EBNA1 transcripts seen at 2 dpi of Sh-Sy5y were much greater than those seen in PBMCs, suggesting a more rapid increase in EBV genome copy numbers or EBNA1 DNA in Sh-Sy5y cells than in PBMCs at 2 dpi but a plateau by 9 dpi.

ACV inhibits EBV genome replication in Sh-Sy5y cells and PBMCs. We used ACV to determine if we could block lytic replication and production of EBV progeny in infected neuronal cells. To see if there is a significant difference between the virus created by EBV replication in Sh-Sy5y neuronal cells and that created by induction of lytic replication of EBV-transformed LCL1 cells, we treated infected cells with ACV after 48 h of induction and used the supernatant collected to infect fresh cells.

The results were similar whether the viruses were produced from Sh-Sy5y or LCL1 cells treated with ACV (Fig. 6E and F). Sh-Sy5y cells were infected with virus collected from GFP-EBV-producing Sh-Sy5y and LCL1 cells treated or not treated with ACV (Fig. 6E and F). Similar GFP signals were seen after infection without ACV at 2 and 5 dpi (Fig. 6, compare panels E and F, ACV−). Furthermore, supernatant generated from cells treated with ACV also had similar signal levels, which were dramatically lower than those obtained with the virus generated from cells not treated with ACV (Fig. 6, compare panels E and F, ACV+). Also, the degree of cell lysis was greatly reduced in Sh-Sy5y cells infected with lysates from ACV-treated Sh-Sy5y and LCL1 cells induced to produce virus. This was expected, as less virus production would result in lower infection efficiency and a reduced overall change in cell lysis due to infection. To corroborate the infection results described above with the direct viral genome copy numbers as a result of treatment with ACV, we collected viral supernatants from treated and untreated cells, extracted viral DNA, and performed a qPCR assay. The results showed that supernatants collected at 2 dpi from ACV-treated cells had similar reductions in GFP-EBV genome copy numbers whether they were generated from Sh-Sy5y or LCL1 cells, with a drop of approximately 40 to 50% (Fig. 6, compare panels G and H). Therefore, ACV affected the lytic replication of GFP-EBV in both Sh-Sy5y and LCL1 cells at similar levels, suggesting inhibition, as expected for herpesviruses.

KSHV infects neuronal cells similarly to EBV. To determine if KSHV, the other known human gammaherpesvirus, can infect neuronal cells similarly to EBV, we exposed Sh-Sy5y cells to recombinant KSHV expressing GFP, GFP-KSHV. After initial infection, cells were monitored by fluorescence microscopy at different time intervals. Cells were collected, and RNA was extracted to determine the expression of viral genes by RT-qPCR assay. Sh-Sy5y neuroblastoma cells showed GFP expression as early as 1 dpi (Fig. 7A and B). This demonstrated that KSHV was able to successfully infect these neuronal cells. Additionally, the viral genome was being transcribed and translated. Like EBV infection, KSHV infection led to changes in the morphology of Sh-Sy5y cells, which was distinct from that of uninfected cells (Fig. 7A and B). LANA (Fig. 7A)- and K8 (Fig. 7B)-specific immunofluorescence showed that by 24 h (1 dpi), both LANA and K8 signals were clearly detected and remained to 9 dpi. Interestingly, the K8 signal was striking, with intense punctate localization at the membrane and neural processes, while LANA localization was predominantly nuclear (Fig. 7A and B).

Total RNA was collected from the cells and reverse transcribed to cDNA before a qPCR assay of the cDNA extracted from Sh-Sy5y cells was carried out. The genes amplified were the KSHV latent gene for LANA and the KSHV lytic gene for K8 (24, 26). GAPDH and 18S rRNAs were used as endogenous controls. As shown in Fig. 7C, LANA showed significant expression by 3 dpi, with a low

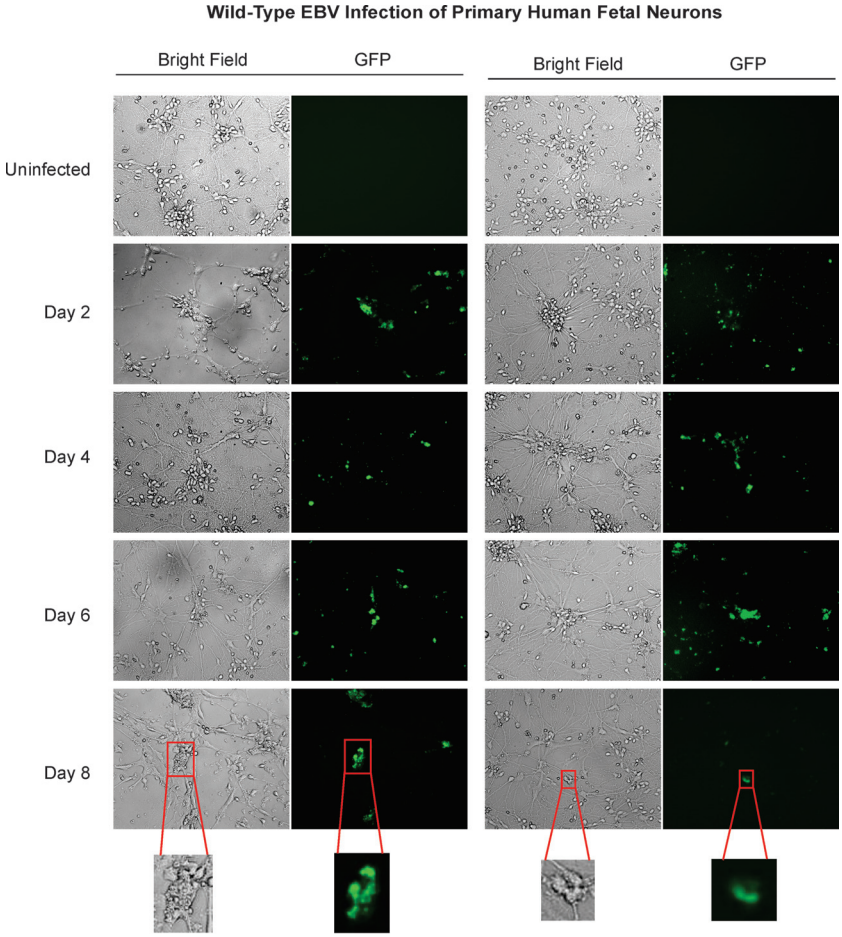

FIG 3 Wild-type EBV infection of primary human fetal neurons. Primary neurons were plated in six-well plates at 90% confluence and infected in the same manner as NT-2 neurons with the appropriate complete neurobasal culture medium. Fluorescence microscopy was carried out at 2, 4, 6, and 8 dpi to monitor for GFP expression. Microscopy images were captured at ×20 magnification.

level detected at 1 dpi. This confirmed the infection of Sh-Sy5y cells. However, and interestingly, from 3 dpi onward, K8 displayed a significant increase in levels of transcription, which continued to increase up to 9 dpi, supporting our observation of lytic replication and similar to the EBV results described above (Fig. 7C). To monitor productive virus induction during Sh-Sy5y infection, we collected infected cell supernatant, purified the virus via centrifugation, and infected fresh Sh-Sy5y cells with virus obtained at 2, 5, and 9 dpi. Interestingly, we showed that the supernatant collected contained virus that was able to infect fresh cells. This experiment supported our claim of active viral progeny production after KSHV infection of neuronal cells.

DISCUSSION

Our work was initiated to broadly determine whether the human oncogenic gammaherpesviruses EBV and KSHV are capable of infecting neuronal cells and to characterize the infection in terms of viral gene expression during infection. A previous study showed that EBV was detected in infected B cells and lymphocytes in the CNS (63, 64). To date, studies have not clearly established EBV or KSHV infection of neuronal cells. The data presented in this report demonstrate that EBV and KSHV are able to effectively infect neuronal cell lines, as well as primary neurons. This phenomenon may potentially provide clues to their contribution to the pathogenesis of human neural diseases. Nonetheless, these viruses may exist in the perfect microenvironment after initiation of the associated pathologies.

Fluorescence microscopy, along with qPCR assay results, demonstrated neuronal cell infection with recombinant GFP-tagged virus. In different neuronal cell lines, we showed infection by GFP signal detection as early as 1 dpi. In Sh-Sy5y cells, the expression of GFP was visualized in the cell bodies and neural processes of infected cells. As the infection progressed, the cells became swollen and eventually underwent lysis, most likely because of virion progeny production. Therefore, EBV and KSHV were undergoing lytic replication to produce progeny virus in this cell type. The RT-qPCR and WB data for Sh-Sy5y cells support our hypothesis, as levels of EBV lytic glycoprotein gp350 and KSHV lytic antigen K8 increased as the infection proceeded. The results of our immunofluorescence assays demonstrated that EBV and KSHV infections had occurred and that during infection of neuronal cells, their lytic programs were activated. EBNA1 protein was clearly present in the nuclei of Sh-Sy5y cells by 2 dpi. This confirmed that EBV genes were produced in the infected cells. WB confirmed the presence of latent EBNA1 and lytic BZLF-1 in EBV-infected Sh-Sy5y cells. This suggested activation of full-blown lytic replication

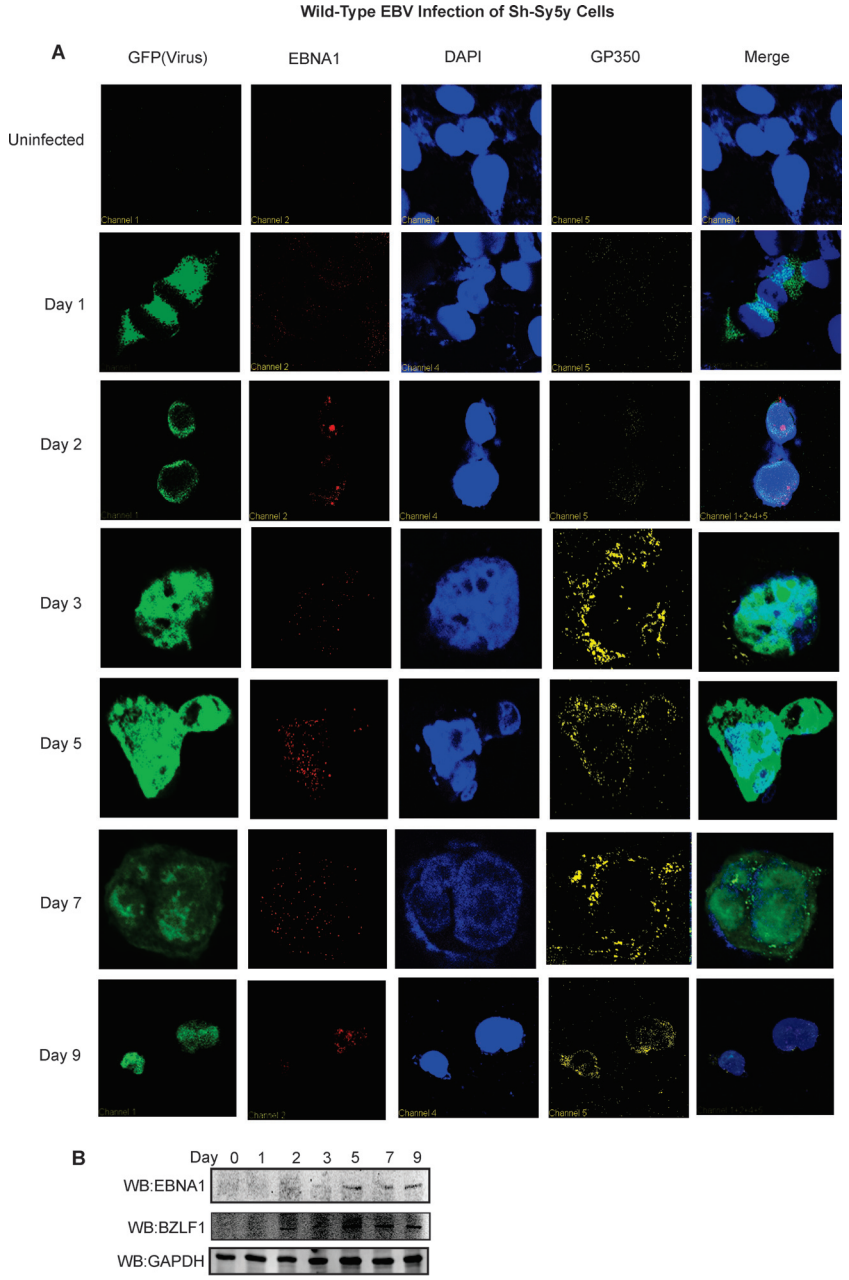

FIG 4 EBV infection of Sh-Sy5y cells produces viral latent and lytic antigen. Sh-Sy5y cells were grown on 100-mm culture plates. At 60% confluence, in addition to the culture medium, 110 μl (~6 × 10^{12} viral copies) of concentrated EBV was added to each plate with 5 μl of Polybrene at a 20-μmol/ml concentration. Control cells were supplemented with only medium and Polybrene. (A) Confocal microscopy was carried out at 1, 2, 3, 5, 7, and 9 dpi with primary antibodies to EBNA1, gp350, and DAPI. Secondary antibodies were used as described in Materials and Methods. (B) Cells were harvested at 1, 2, 3, 5, 7, and 9 dpi for WB analyses with primary antibodies to EBNA1, BZLF1, and GAPDH, which were performed and scanned with an Odyssey infrared scanner (LI-COR Biosciences, Lincoln, NE). Microscopy images were captured at ×60 magnification.

of the viruses in this cell line. Interestingly, a number of clinical findings, such as the presence of EBV in the CSF and nervous systems of affiliated patients, support our finding that these viruses can infect neuronal cells (64, 65). Moreover, at 9 dpi, the infected cells underwent lysis, most likely because of virus progeny generation, and this will be further investigated. Also, at 9 dpi, the population of infected cells was dramatically reduced and it was not monitored further. However, ongoing studies will explore the long-term survival of any of them in culture.

In our NT-2 neuronal cell infection results clearly support those obtained with Sh-Sy5y cells. There was significant GFP expression by 1 dpi. However, the entirety of the neural clusters did not show GFP expression at that time point. Only the cells on the outer rim or periphery of the clusters were GFP positive and so were infected. This was seen more clearly at 3 dpi, as the infection migrated to cells at the center of the neural clusters, and by 6 dpi, the entire clusters were infected. The majority of the cells were dead by 9 dpi, suggesting cell lysis due to lytic infection and viral

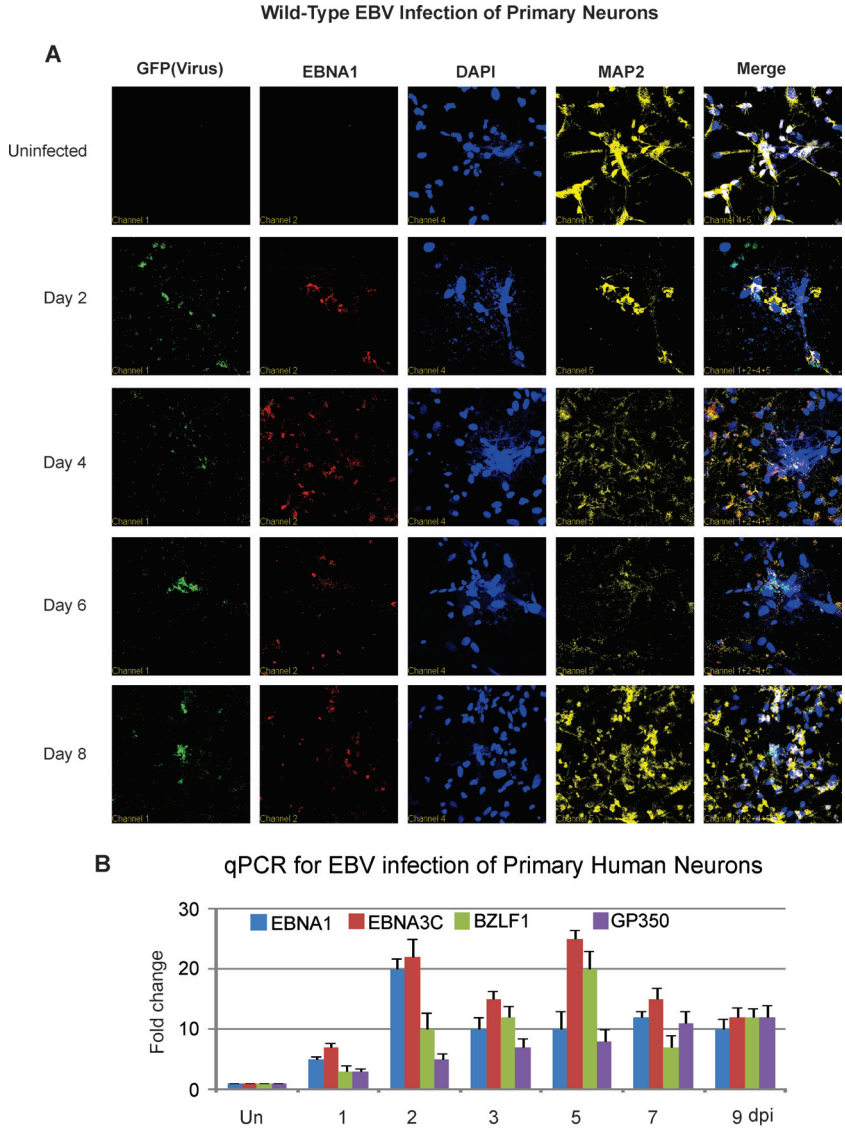

FIG 5 EBV infection of primary neurons results in production of viral transcripts and antigens. (A) Immunofluorescence assays by confocal microscopy were carried out at 2, 4, 6, and 8 dpi with primary antibodies to EBNA1, MAP2, and DAPI for nuclear staining. (B) Analyses for transcripts of EBV genes, namely, those for EBNA1, EBNA3C, BZLF1, and gp350, were carried out 1, 2, 3, 5, 7, and 9 dpi. Un, uninfected. (C) Immunofluorescence assays by confocal microscopy were carried out at 2, 4, 6, and 8 dpi with primary antibodies to gp350, MAP2, and DAPI for nuclear staining.

production, similar to that seen in Sh-Sy5y cell infection. The fact that the virus spread into the neural clusters also supported the lytic-program hypothesis. This progressive infection of NT-2 clusters from the rim to the center is likely to occur if the infected cells on the periphery produced virus. The process was well organized and likely created a special niche for virus production to support the infection of new cells. Studying these processes at the molecular level would prove insightful regarding viral progression in neural environments and how it may differ from B cells and epithelial cells. Further, the transcript data, as quantified by the RT-qPCR assay, confirmed infection after demonstrating the expression of EBNA1, EBNA3C, and LANA, as well as the lytic markers gp350, BZLF1, and K8. The fact that the lytic markers continued to increase supported lytic replication. Furthermore, production of viral progeny capable of infecting fresh cells strongly supported lytic replication with progeny production. Evaluation of cellular factors important for supporting lytic replication will be one of our future studies to understand this process.

The use of primary human fetal neurons in this study was critical, as it represented a more direct physiological link to EBV infection associated with neuronal pathologies. The primary human fetal neuron infection data obtained further support our conclusions about the cell lines. The fluorescence patterns, cell lysis, and viral transcription data postinfection were similar to the trends seen in the Sh-Sy5y cell line. The RT-qPCR and immunofluorescence data both showed increases in lytic gp350 activity, suggesting that EBV undertook a predominantly lytic infection *in vitro*.

Similar to the EBV studies, microscopy, immunofluorescence assay, and viral transcription data also supported KSHV infection of neuronal cells. Further, supernatant from EBV-infected Sh-Sy5y cells was effectively used to infect EBV-negative Sh-Sy5y cells, as well as PBMCs, which demonstrated that the initially in-

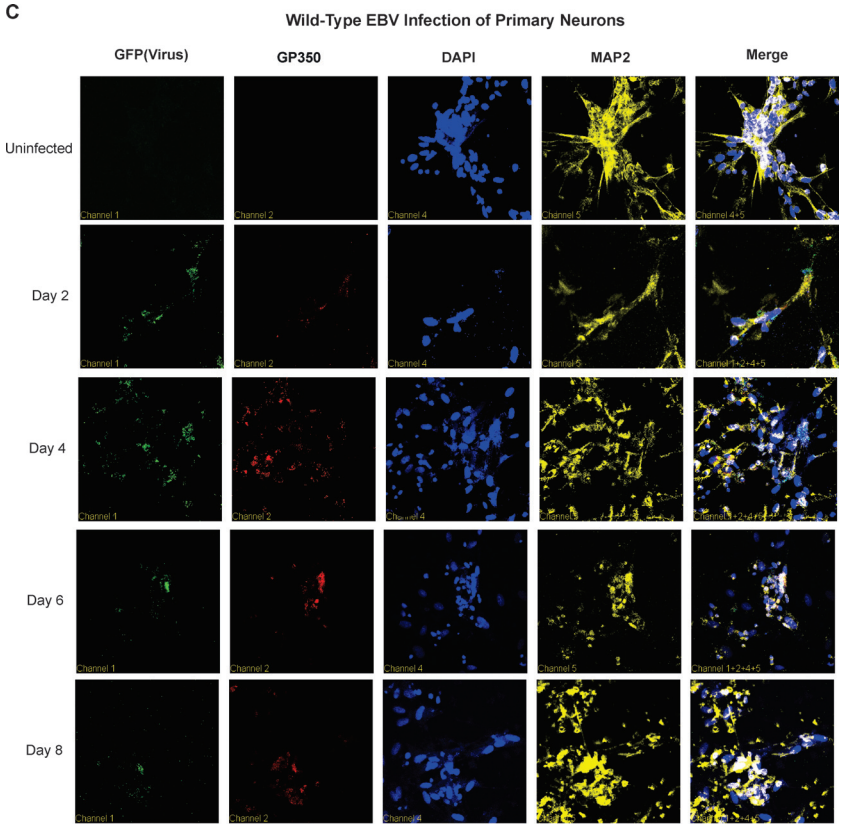

FIG 5 continued

fected Sh-Sy5y cells were producing EBV virions, resulting in cell lysis. We also determined the efficacy of virus produced by infected neuronal cells compared to that of induced virus from EBV-transformed LCL1 cells. ACV-treated Sh-Sy5y cells and induced LCL1 cells showed a strong reduction of virus production for both viral preparations in similar manners, as determined by infection of fresh cells and genome copy numbers. Therefore, viral lytic replication was inhibited in Sh-Sy5y neuronal cells in a manner similar to that seen in LCL1, a B-cell line.

Furthermore, future studies examining the electrochemical signals in EBV- and KSHV-infected neurons compared to unaffected neurons will provide additional clues to these infections in neuronal diseases. In many debilitating neurodegenerative diseases, including MS, the efficiency of electrochemical signals is greatly reduced, often leading to problems related to cognition and muscular activity. It is likely that viral infection with EBV or KSHV may severely reduce these signals, leading to reduced cognition and reduced neuromuscular function. Additionally, patients with EBV- or KSHV-associated cancers may also have additional complications due to infection of neuronal cells, leading to cognitive deficiencies.

This study clearly established that lytic EBV and KSHV infections of neuronal cells resulting in progeny production are possible. However, further studies are required to fully understand the mechanism of these infections and their relevance to neuronal diseases. Our hope is that these studies will persuade the scientific community to take a more in-depth look at neurological pathologies, which may elucidate a role for these ubiquitous gammaherpesviruses as contributors to these pathologies specifically as it may relate to a lytic type of infection. These results also clearly show that infection of neuronal cells can occur. However, it should be clearly stated that they are not supportive of a causative role. They merely provide additional evidence demonstrating their presence. It is also possible that infection may occur after the initiation of these pathologies. Clearly, there is a great deal more to do in this arena.

MATERIALS AND METHODS

Cell and virus cultures. The Sh-Sy5y neuroblastoma cell line was obtained from Ian Blair (Perelman School of Medicine, University of Pennsylvania). This EBV- and KSHV-negative cell line was cultured in Dulbecco's modified Eagle's medium (DMEM) supplemented with 10% fetal bovine serum (FBS), 50 mg/ml streptomycin, and 50 U of penicillin. The cells were grown in 100-mm plates. Coverslips treated with poly-L-lysine (Sigma-Aldrich, St. Louis, MO) were used for immunofluorescence experiments.

Neuron-committed NT-2 cells were obtained from Dennis Kolson (Perelman School of Medicine, University of Pennsylvania). The virus-negative undifferentiated cells were grown in DMEM with 10% FBS supplemented with 50 mg/ml streptomycin and 50 U of penicillin. The cells were differentiated into NT-2 neurons in six-well plates over a span of 6 weeks and maintained as described by Chen et al. (63).

Primary human neurons were obtained from the Temple University School of Medicine Comprehensive NeuroAIDS Center as deidentified culture and maintained in neurobasal medium supplemented with 2% glutamine, 0.4% gentamicin, and 2% B27 supplement. The virus-negative neurons were maintained in six-well plates and in four-well chamber slides for immunofluorescence experiments.

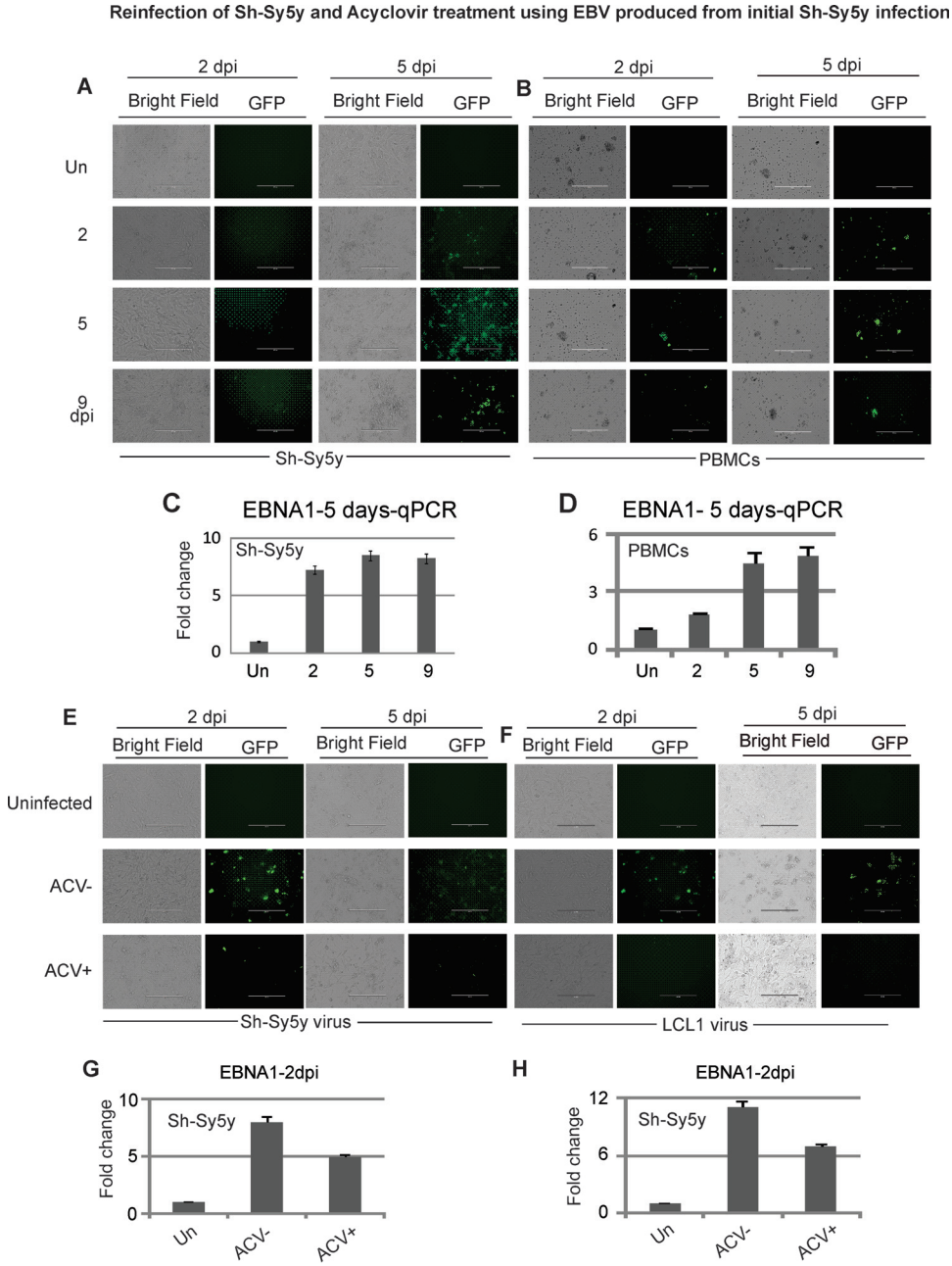

FIG 6 ACV treatment inhibits EBV production in GFP-EBV-producing Sh-Sy5y and LCL1 cells. (A to D) Medium suspensions were collected from infected Sh-Sy5y cultures at 2, 5, and 9 dpi. Sh-Sy5y cells were grown to 60% confluence in six-well plates. For infection, each well was supplemented with 2 ml of complete culture medium, and 200 μl of supernatant collected on day 2, 5, or 9 was added to respective wells with 1 μl of Polybrene. (A and B) Fluorescence microscopy of Sh-Sy5y cells and PBMCs was carried out temporally. (C and D) Transcript analyses of Sh-Sy5y cells and PBMCs were carried by RT-qPCR out at the time points shown. (E to H) Infected Sh-Sy5y cells that were viable after primary infection with GFP-EBV from the HEK293T source cells were selected for by using puromycin at 1 μg/ml of culture medium. GFP-EBV was induced by the same method as HEK293T cells containing BACGFP-EBV. LCL1 cells containing BACGFP-EBV were also cultured and induced. Viruses from both of the sources were concentrated. Sh-Sy5y cells were cultured in six-well plates and infected with GFP-EBV from supernatant obtained from both Sh-Sy5y and LCL1 cells by adding 150 μl of the respective virus supernatant to each well containing 2 ml of complete culture medium and 1 μl of Polybrene. For each virus category, half of the infected cells were supplemented with 25 mM ACV. After 18 h, the infection medium was replaced with fresh medium and ACV was still administered to the ACV-positive group. The extent of infection of Sh-Sy5y cells by GFP-EBV from LCL1 or Sh-Sy5y cells in the presence or absence of ACV was monitored by fluorescence microscopy (E and F), transcript analysis by RT-qPCR assay was performed (G and H), and the results are presented as fold changes. Un, uninfected.

Deidentified human PBMCs were obtained from the University of Pennsylvania Human Immunology Core. These EBV-negative cells were cultured in RPMI 1640 with 7% FBS supplemented with 50 mg/ml streptomycin and 50 U of penicillin. The cells were cultured in six-well plates.

HEK293T cells containing recombinant BACGFP-EBV, an EBV episome expressing GFP and enabling puromycin resistance, were created previously as explained by Halder et al. (52). BACGFP-KSHV was previously described (65, 66). The cells were cultured in DMEM with 5% FBS

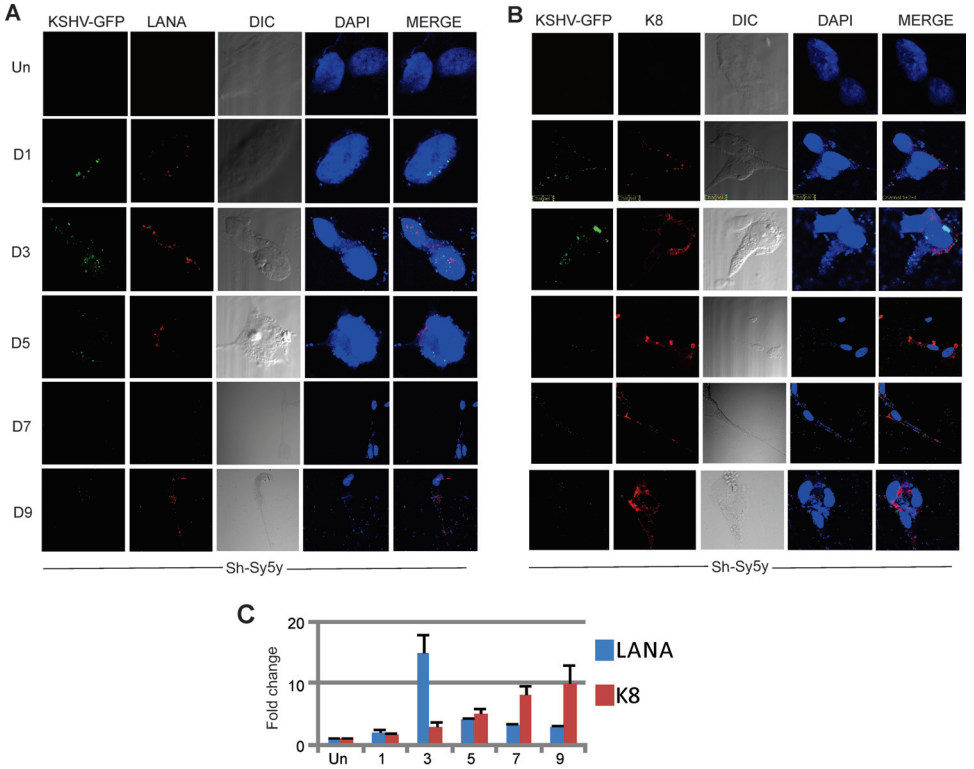

FIG 7 Wild-type KSHV infection of Sh-Sy5y cells. Sh-Sy5y cells were grown in 100-mm culture plates. At 60% confluence, in addition to the culture medium, 110 μl (~6.2 × 10^{12} viral copies) of concentrated KSHV was added to each plate with 5 μl of Polybrene at a 20-μmol/ml concentration. Control cells were supplemented with only medium and Polybrene. (A and B) Confocal microscopy was carried out at 1, 3, 5, 7, and 9 dpi with primary antibodies against LANA, K8, and DAPI. Secondary antibodies were used as described in Materials and Methods. (C) Cells were harvested at 1, 3, 5, 7, and 9 dpi for detection of LANA, K8, and endogenous 18S rRNA transcripts.

supplemented with 50 mg/ml streptomycin, 50 U of penicillin (medium), and 1 μg/ml puromycin. Cells were grown in 175-cm^2 culture flasks.

LCL1 cells containing BACGFP-EBV were created previously (52). The cells were cultured in RPMI 1640 with 7% FBS supplemented with 50 mg/ml streptomycin, 50 U of penicillin (medium), and 1 μg/ml puromycin. Cells were grown in 175-cm^2 culture flasks. All cells were incubated at 37°C with 5% CO_2. The medium of all of the cell lines was changed every 3 days.

Induction of virus from HEK293T cells containing BACGFP-EBV and BACGFP-KSHV. Cells containing BACGFP-EBV or BACGFP-KSHV were induced to release virus by culturing for 5 days in complete DMEM containing 20 ng/ml phorbol ester TPA and 3 mM butyric acid (Sigma-Aldrich, St. Louis, MO). All of the procedures used were described earlier (67, 68). Cell suspensions were centrifuged at 2,100 rpm for 15 min, and the virus-containing supernatant was filtered through a 0.45-μm cellulose acetate filter. The virus was concentrated by ultracentrifugation at 27,000 rpm at 4°C and stored at −80°C.

Infection of Sh-Sy5y cells with GFP-EBV and GFP-KSHV. Sh-Sy5y cells were grown in 100-mm culture plates. For immunofluorescence assays, poly-L-lysine-coated coverslips were placed in the culture plates. At 60% confluence, in addition to the culture medium, virus was added to each plate with 5 μl of Polybrene at 20 μmol/ml. Control cells were supplemented with only medium and Polybrene. Cells were incubated for 18 h, and the medium was replaced with fresh complete DMEM. Medium was collected and changed at 2, 5, and 9 dpi. Fluorescence microscopy was carried out at similar intervals to monitor GFP expression. Cells were harvested at these time points for gene expression analysis.

Infection of NT-2 neurons with GFP-EBV obtained from infected HEK293T cells. NT-2 neurons were differentiated in six-well plates to a density of 700 to 900 neural clusters per well. In addition to 2 ml of complete culture medium per well, a virus suspension in VIM (virus infection medium) was added to each well. Polybrene was not used for this infection. Control neurons were supplemented with medium only. The medium was swapped with fresh complete culture medium after 18 h. Thereafter, the medium was changed every 3 days. Fluorescence microscopy was carried out at 1, 3, 5, 7, and 9 dpi to monitor GFP expression. Neurons were harvested thereafter for gene expression analysis.

Infection of primary neurons with GFP-EBV obtained from infected HEK293T cells. Primary neurons were plated in six-well plates at 90% confluence and infected in the same manner as NT-2 neurons with the appropriate complete neurobasal culture medium (69). Fluorescence microscopy was carried out at 2, 4, 6, and 8 dpi to check for GFP expression, and the neurons were harvested at the appropriate time points for gene expression analysis. These cells were harvested 48 h postinfection instead of at 24 h postinfection, as their growth rate was lower than that of the other cell lines used.

DNA and RNA extraction. For quantitation of intracellular viral DNA, cells were harvested and washed twice with 1× phosphate-buffered saline (PBS) to remove the residual virus. Cells were incubated in HMW buffer (10 mM Tris-HCl [pH 8.0], 150 mM NaCl, 10 mM EDTA, 0.5% SDS) for 2 h at 55°C. Five hundred micrograms per milliliter proteinase K was added, and the mixture was incubated at 37°C overnight with subsequent extraction by the phenol-chloroform-isopropanol method. Viral DNA was treated with RNase, precipitated, and then resuspended in water. Extracellular viral DNA was extracted from culture supernatants as described previously (70, 71). In brief, virions were pelleted at 70,000 × *g* for 2 h at 4°C and resuspended. Cellular DNAs and free viral DNAs were removed by treatment with DNase I at 37°C. Virion DNA was treated with HMW buffer for 20 min (63, 64). This was followed by treatment with proteinase K overnight at 37°C and subsequent extraction by the phenol-

TABLE 1 Primers used for RT-qPCR

Primer and strand	DNA sequence (5′–3′)	Reference
EBNA1		
Forward	CACCATTGAGTCGTCTCCCC	52
Reverse	TCAAAGCTGCACACAGTCAC	
EBNA3C		
Forward	AGAAGGGGAGCGGTGTTGTG	52
Reverse	ACGGCAGGAGGCCCAGTATC	
gp350		
Forward	AGGTGCTGCAGCCCTCGAGGAAGTC	52
Reverse	GGCTAGCGAGAATCCATCACCGACT	
BZLF1		
Forward	AACCGCTCCGACTGGGTCGTGGTTT	52
Reverse	CCAGGTTGAGGTGCTTCTCCCCCGG	
LANA		
Forward	CCATCTCTTGCATTGCCAC	60
Reverse	AACTACGGTTGGCGAAGTCA	
K8		
Forward	TTCGCGTGGGAGAATGTGA	57
Reverse	ACAGCCCACACATGTCCTGT	
GADPH		
Forward	ACGACCACTTTGTCAAGCTC	60
Reverse	GGTCTACATGGCAACTGTGA	
18S rRNA		
Forward	GGCCCTGTAATTGGAATGAGTC	52
Reverse	CCAAGATCCAACTACGAGCTT	

chloroform-isopropanol method. Intracellular and extracellular viral DNA preparations were quantitated by RT-qPCR assays for EBNA1, EBNA3C, and gp350 for EBV and LANA and K8 for KSHV with previously described primers (52, 57, 60).

Real-time PCR assays. To determine the intracellular viral RNA, we extracted the total RNA from ~6×10^6 to 8×10^6 GFP-EBV- or GFP-KSHV-infected Sh-Sy5y cells, NT-2 neurons, primary human neurons, or PBMCs at the specified time points postinfection with the TRIzol reagent (Invitrogen Inc., Carlsbad, CA) as described earlier (72). A 1.0-μg sample of DNase-treated total RNA was used to synthesize cDNA with the high-capacity RNA-cDNA kit (Applied Biosystems Inc., Foster City, CA) according to the manufacturer's instructions. The specific target gene for amplification are shown in Table 1. The target genes were amplified from cDNA with power SYBR green PCR master mix (Applied Biosystems Inc., Carlsbad, CA), 1 mM primer, and 2 μl of the cDNA product in a total volume of 10 μl. The reactions were prformed with 96-well plates at 95°C for 10 min, followed by 36 cycles of 95°C for 30 s, 56°C for 30 s, and 72°C for 30 s and then 10 min at 72°C. Melting curve analysis was performed to verify the specificity of the amplified products. The relative quantitation values were calculated by the $\Delta\Delta C_T$ method. All reactions were run in triplicate. GAPDH was used as the endogenous control.

Immunofluorescence assay. Sh-Sy5y cells were grown and infected directly on 22-by-22-mm coverslips. At specified time points, the coverslips were washed with PBS and fixed for 30 min with 4% paraformaldehyde with 0.1% Triton X-100. Cells were washed again in PBS and blocked with 3% milk prepared in PBS for 30 min. The coverslips were washed twice with PBS, and primary staining was done overnight with rabbit anti-EBNA1 (10 μg/ml, 1:1,000 dilution), anti-LANA (1:200), anti-K8 (1:200), and anti-gp350 (1:200) mouse hybridoma supernatant. The coverslips were washed three times with PBS, and secondary staining was done for 1 h with goat anti-rabbit antibody (595 nm, 1:1,000 dilution), donkey anti-mouse antibody (647 nm, 1:1,000 dilution), and DAPI antibody (1:500 dilution). Coverslips were washed three times with PBS and mounted on slides with antifade (Molecular Probes Inc., Carlsbad, CA).

Primary human neurons were prepared and infected in four-well chamber slides. For the times specified, the cells were washed with PBS and fixed for 30 min with 4% paraformaldehyde with 0.1% Triton X-100. Cells were washed again in PBS and blocked with 3% milk prepared in PBS for 30 min. Coverslips were washed twice with PBS, and primary staining was done overnight with chicken anti-MAP2 antibody (19 μg/ml, 1:10,000 dilution) and rabbit anti-EBNA1 antibody (1:1,000 dilution) or anti-gp350 mouse hybridoma supernatant. The slides were washed three times with PBS, and secondary staining was done for 1 h with goat anti-chicken antibody (650 nm, 1:2,000 dilution), DAPI antibody (1:500), and either goat anti-rabbit antibody (595 nm, 1:1,000 dilution) or donkey anti-mouse antibody (595 nm, 1:1,000 dilution). Slides were washed three times with PBS mounted onto coverslips with antifade. Fluorescence was viewed by confocal microscopy and analyzed with the Fluoview 300 software (Olympus Inc., Melville, NY).

Infection assays with EBV produced from initial Sh-Sy5y cell GFP-EBV infection. Medium suspensions were collected from infected Sh-Sy5y cell cultures. Suspensions were centrifuged at 2,100 rpm for 15 min, and the virus-containing supernatant was filtered through a 0.45-μm cellulose acetate filter. The virus was concentrated by ultracentrifugation at 27,000 rpm at 4°C and stored at −80°C. Sh-Sy5y cells were grown to 60% confluence in six-well plates. For infection, each well was supplemented with 2 ml of complete culture medium and 200 μl of virus was collected at different time points and added to respective wells with 1 μl of Polybrene. Infection medium was replaced with fresh medium after 18 h. Fluorescence microscopy and genetic analysis by real-time PCR were carried out at specified time points. PBMCs were infected with virus in the same manner as described earlier.

Infection of cells with GFP-EBV obtained from ACV-treated Sh-Sy5y and LCL1 cells. Sh-Sy5y cells infected with GFP-EBV from HEK293T cells used to stably maintain the virus were selected with 1 μg/ml puromycin. Infected Sh-Sy5y cells were induced by the same method as the HEK293T cells containing GFP-EBV described above. LCL1 cells containing GFP-EBV were also cultured and freshly induced at the same time. Viruses from both sources were harvested and concentrated as described above. Sh-Sy5y cells were cultured in six-well plates and infected with purified virus from GFP-EBV-producing Sh-Sy5y and LCL1 cells by adding 150 μl of the respective virus preparations to each well containing 2 ml of complete culture medium and 1 μl of Polybrene. For each virus category, half of the infected cells were supplemented with 25 mM ACV. After 18 h, the infection medium was replaced with fresh medium but ACV was still administered to the ACV-positive group. The extent of infection of Sh-Sy5y cells by either LCL1 or Sh-Sy5y GFP-EBV in the presence or absence of ACV was monitored by fluorescence microscopy and RT-qPCR analysis.

WB. Cells were harvested, washed with ice-cold PBS, and then lysed with radioimmunoprecipitation assay buffer (10 mM Tris [pH 7.5], 150-mM sodium chloride, 2 mM EDTA, 1% NP-40). A protease inhibitor cocktail was added before lysis of the cells. The cell debris was removed by centrifugation at 21,000 $\times$ *g* for 12 min (4°C), and the supernatant was transferred into sterile microcentrifuge tubes. The lysates were then quantitated and normalized. WB was performed as described previously (67).

ACKNOWLEDGMENTS

We thank Ian Blair of the Perelman School of Medicine at the University of Pennsylvania for generously providing the Sh-Sy5y cell line. We also acknowledge the Comprehensive NeuroAIDS Center (P30 MH09217) at the Temple University School of Medicine and Kamel Khalili for providing the primary human fetal neurons. We also thank the Pathology Department at the Perelman School of Medicine at the University of Pennsylvania for supplying the splenic tissues. Additionally, we thank the Human Brain and the Spinal Fluid Resource Center at the University of California Los Angeles for supplying brain tissue samples. Special thanks to all Robertson lab members for helpful discussion and technical help.

This project was supported by Public Health Service grants R01-CA-137894, R01-CA-171979, R01-CA-177423, CA-137894-05, P30-DK-050306, and P01-CA-174439 to Erle S. Robertson. Erle S. Robertson is a scholar of the Leukemia and Lymphoma Society of America.

REFERENCES

1. **Tao Q, Young LS, Woodman CB, Murray PG.** 2006. Epstein-Barr virus (EBV) and its associated human cancers—genetics, epigenetics, pathobiology and novel therapeutics. Front Biosci **11:**2672–2713. http://dx.doi.org/10.2741/2000.
2. **Maeda E, Akahane M, Kiryu S, Kato N, Yoshikawa T, Hayashi N, Aoki S, Minami M, Uozaki H, Fukayama M, Ohtomo K.** 2009. Spectrum of Epstein-Barr virus-related diseases: a pictorial review. Jpn J Radiol **27:**4–19. http://dx.doi.org/10.1007/s11604-008-0291-2.
3. **Küppers R.** 2003. B cells under influence: transformation of B cells by Epstein-Barr virus. Nat Rev Immunol **3:**801–812. http://dx.doi.org/10.1038/nri1201.
4. **Rickinson AB, Kieff E.** 2001. Epstein-Barr virus. In Knipe DM, Howley GD, Lamb RA, Martin MA, Roizman B, Straus SE (ed), Fields virology. Lippincott Williams & Wilkins: Philadelphia, PA.
5. **Sixbey JW, Davis DS, Young LS, Hutt-Fletcher L, Tedder TF, Rickinson AB.** 1987. Human epithelial cell expression of an Epstein-Barr virus receptor. J Gen Virol **68:**805–811. http://dx.doi.org/10.1099/0022-1317-68-3-805.
6. **Baumforth KR, Young LS, Flavell KJ, Constandinou C, Murray PG.** 1999. The Epstein-Barr virus and its association with human cancers. Mol Pathol **52:**307–322. http://dx.doi.org/10.1136/mp.52.6.307.
7. **Jones JF, Shurin S, Abramowsky C, Tubbs RR, Sciotto CG, Wahl R, Sands J, Gottman D, Katz BZ, Sklar J.** 1988. T-cell lymphomas containing Epstein-Barr viral DNA in patients with chronic Epstein-Barr virus infections. N Engl J Med **318:**733–741. http://dx.doi.org/10.1056/NEJM198803243181203.
8. **Amon W, Farrell PJ.** 2005. Reactivation of Epstein-Barr virus from latency. Rev Med Virol **15:**149–156. http://dx.doi.org/10.1002/rmv.456.
9. **Ebell MH.** 2004. Epstein-Barr virus infectious mononucleosis. Am Fam Physician **70:**1279–1287.
10. **Thompson MP, Kurzrock R.** 2004. Epstein-Barr virus and cancer. Clin Cancer Res **10:**803–821. http://dx.doi.org/10.1158/1078-0432.CCR-0670-3.
11. **Brady G, Macarthur GJ, Farrell PJ.** 2008. Epstein-Barr virus and Burkitt lymphoma. Postgrad Med J **84:**372–377. http://dx.doi.org/10.1136/jcp.2007.047977.
12. **Takada K.** 2001. Role of Epstein-Barr virus in Burkitt's lymphoma. Curr Top Microbiol Immunol **258:**141–151. http://dx.doi.org/10.1007/978-3-642-56515-1_9.
13. **Parravicini C, Chandran B, Corbellino M, Berti E, Paulli M, Moore PS, Chang Y.** 2000. Differential viral protein expression in Kaposi's sarcoma-associated herpesvirus-infected diseases: Kaposi's sarcoma, primary effusion lymphoma, and multicentric Castleman's disease. Am J Pathol **156:**743–749. http://dx.doi.org/10.1016/S0002-9440(10)64940-1.
14. **Parravicini C, Chandran B, Corbellino M, Berti E, Paulli M, Moore PS, Chang Y.** 2000. Differential viral protein expression in Kaposi's sarcoma-associated herpesvirus-infected diseases: Kaposi's sarcoma, primary effusion lymphoma, and multicentric Castleman's disease. Am J Pathol **156:**743–749. http://dx.doi.org/10.1016/S0002-9440(10)64940-1.
15. **Janz A, Oezel M, Kurzeder C, Mautner J, Pich D, Kost M, Hammerschmidt W, Delecluse H-.** 2000. Infectious Epstein-Barr virus lacking major glycoprotein BLLF1 (gp350/220) demonstrates the existence of additional viral ligands. J Virol **74:**10142–10152. http://dx.doi.org/10.1128/JVI.74.21.10142-10152.2000.
16. **Tanner J, Weis J, Fearon D, Whang Y, Kieff E.** 1987. Epstein-Barr virus gp350/220 binding to the B lymphocyte C3d receptor mediates adsorption, capping, and endocytosis. Cell **50:**203–213. http://dx.doi.org/10.1016/0092-8674(87)90216-9.
17. **Xiao J, Palefsky JM, Herrera R, Berline J, Tugizov SM.** 2009. EBV BMRF-2 facilitates cell-to-cell spread of virus within polarized oral epithelial cells. Virology **388:**335–343. http://dx.doi.org/10.1016/j.virol.2009.03.030.
18. **Tugizov SM, Berline JW, Palefsky JM.** 2003. Epstein-Barr virus infection of polarized tongue and nasopharyngeal epithelial cells. Nat Med **9:**307–314. http://dx.doi.org/10.1038/nm830.
19. **Bajaj BG, Murakami M, Robertson ES.** 2007. Molecular biology of EBV in relationship to AIDS-associated oncogenesis. Cancer Treat Res **133:**141–162. http://dx.doi.org/10.1007/978-0-387-46816-7_5.
20. **Middeldorp JM, Brink AATP, van den Brule AJC, Meijer CJLM.** 2003. Pathogenic roles for Epstein-Barr virus (EBV) gene products in EBV-associated proliferative disorders. Crit Rev Oncol Hematol **45:**1–36. http://dx.doi.org/10.1016/S1040-8428(02)00078-1.
21. **Sivachandran N, Wang X, Frappier L.** 2012. Functions of the Epstein-Barr virus EBNA1 protein in viral reactivation and lytic infection. J Virol **86:**6146–6158. http://dx.doi.org/10.1128/JVI.00013-12.
22. **Dupin N, Fisher C, Kellam P, Ariad S, Tulliez M, Franck N, van Marck E, Salmon D, Gorin I, Escande J-, Weiss RA, Alitalo K, Boshoff C.** 1999. Distribution of human herpesvirus-8 latently infected cells in Kaposi's sarcoma, multicentric Castleman's disease, and primary effusion lymphoma. Proc Natl Acad Sci U S A **96:**4546–4551. http://dx.doi.org/10.1073/pnas.96.8.4546.
23. **Young LS, Murray PG.** 2003. Epstein-Barr virus and oncogenesis: from latent genes to tumours. Oncogene **22:**5108–5121. http://dx.doi.org/10.1038/sj.onc.1206556.
24. **Cesarman E.** 2011. Gammaherpesvirus and lymphoproliferative disorders in immunocompromised patients. Cancer Lett **305:**163–174. http://dx.doi.org/10.1016/j.canlet.2011.03.003.
25. **Neri A, BarrigabF, Inghirami G, Knowles DM, Neequaye J, Magrath IT, Dalla-Favera R.** 1991. Epstein-Barr virus infection precedes clonal expansion in Burkitt's and acquired immunodeficiency syndrome-associated lymphoma. Blood **77:**1092–1095.
26. **Lacoste V.** 2004. Kaposi's sarcoma-associated herpesvirus immediate early gene activity. Front Biosci **9:**2245–2272. http://dx.doi.org/10.2741/1394.
27. **Cordier-Bussat M, Billaud M, Calender A, Lenoir GM.** 1993. Epstein-Barr virus (EBV) nuclear-antigen-2-induced up-regulation of CD21 and CD23 molecules is dependent on a permissive cellular context. Int J Cancer **53:**153–160. http://dx.doi.org/10.1002/ijc.2910530128.
28. **Fang C, Huang S, Wu C, Hsu H, Chou S, Tsai C, Chang Y, Takada K, Chen J.** 2012. The synergistic effect of chemical carcinogens enhances Epstein-Barr virus reactivation and tumor progression of nasopharyngeal carcinoma cells. PLoS One **7:**e44810. http://dx.doi.org/10.1371/journal.pone.0044810.
29. **Mauser A, Saito S', Appella E, Anderson CW, Seaman WT, Kenney S.** 2002. The Epstein-Barr virus immediate-early protein BZLF1 regulates p53 function through multiple mechanisms. J Virol **76:**12503–12512. http://dx.doi.org/10.1128/JVI.76.24.12503-12512.2002.
30. **MacMahon B.** 1966. Epidemiology of Hodgkin's disease. Cancer Res **26:**1189–1201.
31. **Carbone I, Lazzarotto T, Ianni M, Porcellini E, Forti P, Masliah E, Gabrielli L, Licastro F.** 2014. Herpesvirus in Alzheimer's disease: relation to progression of the disease. Neurobiol Aging **35:**122–129. http://dx.doi.org/10.1016/j.neurobiolaging.2013.06.024.
32. **Lovett-Racke AE, Racke MK.** 2006. Epstein-Barr virus and multiple sclerosis. Arch Neurol **63:**810–811. http://dx.doi.org/10.1001/archneur.63.6.810.
33. **DeLorenze GN, Munger KL, Lennette ET, Orentreich N, Vogelman JH, Ascherio A.** 2006. Epstein-Barr virus and multiple sclerosis: evidence of association from a prospective study with long-term follow-up. Arch Neurol **63:**839–844. http://dx.doi.org/10.1001/archneur.63.6.noc50328.
34. **Munger K, Levin L, O'Reilly E, Falk K, Ascherio A.** 2011. Anti-Epstein-Barr virus antibodies as serological markers of multiple sclerosis: a prospective study among United States military personnel. Mult Scler **17:**1185–1193. http://dx.doi.org/10.1177/1352458511408991.
35. **Kleines M, Schiefer J, Stienen A, Blaum M, Ritter K, Häusler M.** 2011. Expanding the spectrum of neurological disease associated with Epstein-Barr virus activity. Eur J Clin Microbiol Infect Dis **30:**1561–1569. http://dx.doi.org/10.1007/s10096-011-1261-7.
36. **Masajtis-Zagajewska A.** 2012. Guillain-Barre syndrome in the course of EBV infection after kidney transplantation—a case report. Ann Transplant **17:**133–137. http://dx.doi.org/10.12659/AOT.883468.
37. **McCarthy CL, McColgan P, Martin P.** 2012. Acute cerebellar ataxia due to Epstein-Barr virus. Pract Neurol **12:**238–240. http://dx.doi.org/10.1136/practneurol-2011-000115.
38. **Robinson TJ, Glenn MS, Temple RW, Wyatt D, Connolly JH.** 1980. Encephalitis and cerebellar ataxia associated with Epstein-Barr virus infections. Ulster Med J **49:**158–164.
39. **Rubin DI, Daube JR.** 1999. Subacute sensory neuropathy associated with Epstein-Barr virus. Muscle Nerve **22:**1607–1610. http://dx.doi.org/10.1002/(SICI)1097-4598(199911)22:11<1607::AID-MUS21>3.0.CO;2-J.
40. **Gavin C, Langan Y, Hutchinson M.** 1997. Cranial and peripheral neuropathy due to Epstein-Barr virus infection. Postgrad Med J **73:**419–420. http://dx.doi.org/10.1136/pgmj.73.861.419.
41. **Wang J, Ozzard A, Nathan M, Atkins M, Nelson M, Gazzard B, Bower M.** 2007. The significance of Epstein-Barr virus detected in the cerebro-

spinal fluid of people with HIV infection. HIV Med **8:**306–311. http://dx.doi.org/10.1111/j.1468-1293.2007.00475.x.
42. **Weinberg A, Li S, Palmer M, Tyler KL**. 2002. Quantitative CSF PCR in Epstein-Barr virus infections of the central nervous system. Ann Neurol **52:**543–548. http://dx.doi.org/10.1002/ana.10321.
43. **Pender MP**. 2011. The essential role of Epstein-Barr virus in the pathogenesis of multiple sclerosis. Neuroscientist **17:**351–367. http://dx.doi.org/10.1177/1073858410381531.
44. **Fraser K**. 1979. Increased tendency to spontaneous *in vitro* lymphocyte transformation in clinically active multiple sclerosis. Lancet **ii:**175–176. http://dx.doi.org/10.1016/S0140-6736(79)90643-3.
45. **Sumaya CV, Myers LW, Ellison GW**. 1980. Epstein-Barr virus antibodies in multiple sclerosis. Arch Neurol **37:**94–96. http://dx.doi.org/10.1001/archneur.1980.00500510052009.
46. **Pender MP**. 2011. The essential role of Epstein-Barr virus in the pathogenesis of multiple sclerosis. Neuroscientist **17:**351–367. http://dx.doi.org/10.1177/1073858410381531.
47. **Ascherio A**. 2008. Epstein-Barr virus in the development of multiple sclerosis. Expert Rev Neurother **8:**331–333. http://dx.doi.org/10.1586/14737175.8.3.331.
48. **Ascherio A, Munch M**. 2000. Epstein-Barr virus and multiple sclerosis. Epidemiology **11:**220–224. http://dx.doi.org/10.1097/00001648-200003000-00023.
49. **Ascherio A, Munger K**. 2008. Epidemiology of multiple sclerosis: from risk factors to prevention. Semin Neurol **28:**17–28. http://dx.doi.org/10.1055/s-2007-1019126.
50. **Levin LI**. 2003. Multiple sclerosis and Epstein-Barr virus. JAMA **289:**1533–1536. http://dx.doi.org/10.1001/jama.289.12.1533.
51. **Serafini B, Rosicarelli B, Franciotta D, Magliozzi R, Reynolds R, Cinque P, Andreoni L, Trivedi P, Salvetti M, Faggioni A, Aloisi F**. 2007. Dysregulated Epstein-Barr virus infection in the multiple sclerosis brain. J Exp Med **204:**2899–2912. http://dx.doi.org/10.1084/jem.20071030.
52. **Halder S, Murakami M, Verma SC, Kumar P, Yi F, Robertson ES**. 2009. Early events associated with infection of Epstein-Barr virus infection of primary B-cells. PLoS One **4:**e7214. http://dx.doi.org/10.1371/journal.pone.0007214.
53. **Datta AK, Colby BM, Shaw JE, Pagano JS**. 1980. Acyclovir inhibition of Epstein-Barr virus replication. Proc Natl Acad Sci U S A **77:**5163–5166. http://dx.doi.org/10.1073/pnas.77.9.5163.
54. **Lycke J, Svennerholm B, Hjelmquist E, Frisn L, Badr G, Andersson M, Vahlne A, Andersen O**. 1996. Acyclovir treatment of relapsing-remitting multiple sclerosis. A randomized, placebo-controlled, double-blind study. J Neurol **243:**214–224. http://dx.doi.org/10.1007/BF00868517.
55. **Serafini B, Rosicarelli B, Franciotta D, Magliozzi R, Reynolds R, Cinque P, Andreoni L, Trivedi P, Salvetti M, Faggioni A, Aloisi F**. 2007. Dysregulated Epstein-Barr virus infection in the multiple sclerosis brain. J Exp Med **204:**2899–2912. http://dx.doi.org/10.1084/jem.20071030.
56. **Biedler JL, Helson L, Spengler BA**. 1973. Morphology and growth, tumorigenicity, and cytogenetics of human neuroblastoma cells in continuous culture. Cancer Res **33:**2643–2652.
57. **Ross RA, Spengler BA, Biedler JL**. 1983. Coordinate morphological and biochemical interconversion of human neuroblastoma cells. J Natl Cancer Inst **71:**741–747.
58. **Andrews PW, Damjanov I, Simon D, Banting GS, Carlin C, Dracopoli NC, Føgh J**. 1984. Pluripotent embryonal carcinoma clones derived from the human teratocarcinoma cell line tera-2. Differentiation *in vivo* and *in vitro*. Lab Invest **50:**147–162.
59. **Pleasure SJ, Lee VM-**. 1993. NTera 2 cells: a human cell line which displays characteristics expected of a human committed neuronal progenitor cell. J Neurosci Res **35:**585–602. http://dx.doi.org/10.1002/jnr.490350603.
60. **Napoli A, Obeid I**. 18 August 2015. Comparative analysis of human and rodent brain primary neuronal culture spontaneous activity using microelectrode array technology. J Cell Biochem. http://dx.doi.org/10.1002/jcb.25312.
61. **Nuebling C, Buck M, Boos H, Deimling AV, Mueller-Lantzsch N**. 1992. Expression of Epstein-Barr virus membrane antigen gp350/220 in *E. coli* and in insect cells. Virology **191:**443–447. http://dx.doi.org/10.1016/0042-6822(92)90207-6.
62. **Soltani MH, Soltani MH, Pichardo R, Song Z, Sangha N, Camacho F, Satyamoorthy K, Sangueza OP, Setaluri V**. 2005. Microtubule-associated protein 2, a marker of neuronal differentiation, induces mitotic defects, inhibits growth of melanoma cells, and predicts metastatic potential of cutaneous melanoma. Am J Pathol **166:**1841–1850. http://dx.doi.org/10.1016/S0002-9440(10)62493-5.
63. **Chen W, Sulcove J, Frank I, Jaffer S, Ozdener H, Kolson DL**. 2002. Development of a human neuronal cell model for human immunodeficiency virus (HIV)-infected macrophage-induced neurotoxicity: apoptosis induced by HIV type 1 primary isolates and evidence for involvement of the Bcl-2/Bcl-xL-sensitive intrinsic apoptosis pathway. J Virol **76:**9407–9419. http://dx.doi.org/10.1128/JVI.76.18.9407-9419.2002.
64. **Martelius T, Lappalainen M, Palomäki M, Anttila V**. 2011. Clinical characteristics of patients with Epstein-Barr virus in cerebrospinal fluid. BMC Infect Dis **11:**281. http://dx.doi.org/10.1186/1471-2334-11-281.
65. **Jha HC, Lu J, Verma SC, Banerjee S, Mehta D, Robertson ES**. 2014. Kaposi's sarcoma-associated herpesvirus genome programming during the early stages of primary infection of peripheral blood mononuclear cells. mBio **5:**e02261-14. http://dx.doi.org/10.1128/mBio.02261-14.
66. **Brulois KF, Chang H, Lee AS-Y, Ensser A, Wong L-Y, Toth Z, Lee SH, Lee H-R, Myoung J, Ganem D, Oh T-K, Kim JF, Gao S-J, Jung JU**. 2012. Construction and manipulation of a new Kaposi's sarcoma-associated herpesvirus bacterial artificial chromosome clone. J Virol **86:**9708–9720. http://dx.doi.org/10.1128/JVI.01019-12.
67. **Jha HC, Lu J, Saha A, Cai Q, Banerjee S, Prasad MAJ, Robertson ES**. 2013. EBNA3C-mediated regulation of aurora kinase B contributes to Epstein-Barr virus-induced B-cell proliferation through modulation of the activities of the retinoblastoma protein and apoptotic caspases. J Virol **87:**12121–12138. http://dx.doi.org/10.1128/JVI.02379-13.
68. **Jha HC, Upadhyay SK, Aj MP, Lu J, Cai Q, Saha A, Robertson ES**. 2013. H2AX phosphorylation is important for LANA-mediated Kaposi's sarcoma-associated herpesvirus episome persistence. J Virol **87:**5255–5269. http://dx.doi.org/10.1128/JVI.03575-12.
69. **Gordon J, Amini S, White MK**. 2013. General overview of neuronal cell culture. Methods Mol Biol **1078:**1–8. http://dx.doi.org/10.1007/978-1-62703-640-5_1.
70. **Myoung J, Ganem D**. 2011. Active lytic infection of human primary tonsillar B cells by KSHV and its noncytolytic control by activated $CD4^+$ T cells. J Clin Invest **121:**1130–1140. http://dx.doi.org/10.1172/JCI43755.
71. **Lu J, Verma SC, Cai Q, Robertson ES**. 2011. The single RBP-Jkappa site within the LANA promoter is crucial for establishing Kaposi's sarcoma-associated herpesvirus latency during primary infection. J Virol **85:**6148–6161. http://dx.doi.org/10.1128/JVI.02608-10.
72. **Jha HC, Aj MP, Saha A, Banerjee S, Lu J, Robertson ES**. 2014. Epstein-Barr virus essential antigen EBNA3C attenuates H2AX expression. J Virol **88:**3776–3788. http://dx.doi.org/10.1128/JVI.03568-13.